Journal of Magnetism and Magnetic Materials 613 (2025) 172651

Contents lists available at ScienceDirect

Journal of Magnetism and Magnetic Materials

journal homepage: www.elsevier.com/locate/jmmm

Research article

Electron Spin Resonance (ESR) studies on $GdCuBi_2$ intermetallic antiferromagnet

G.S. Freitas [a,b,*], H. Pizzi [a], F.B. Carneiro [b,c], M.H. Carvalho [a,b], E.M. Bittar [b,c], E.D. Bauer [b], J.D. Thompson [b], F. Ronning [b], S.M. Thomas [b], P.F.S. Rosa [b], S.M. Greer [b], P.G. Pagliuso [a,b]

[a] Instituto de Física "Gleb Wataghin", UNICAMP, 13083-859, Campinas, SP, Brazil
[b] Los Alamos National Laboratory, Los Alamos, New Mexico 87545, USA
[c] Brazilian Center for Research in Physics, Rio de Janeiro-RJ, Brazil

ARTICLE INFO

Keywords:
Intermetallic compounds
Gd ESR measurements
Rare-earth antiferromagnetic compound

ABSTRACT

We report temperature dependent X-Band ($\nu \approx 9.5$ GHz) Electron Spin Resonance (ESR) on the $GdCuBi_2$ intermetallic compound. This compound presents a metallic Curie–Weiss paramagnetic behavior at high temperatures and orders antiferromagnetically at $T_N = 14.3$ K. Well above T_N (T > 250 K), the ESR experiments revealed temperature independent g-values spectra composed of a single Dysonian Gd^{3+} ESR line for the studied compound. Within the same temperature range, the Gd^{3+} ESR linewidth ΔH presents a linear broadening temperature dependence known as Korringa behavior. The obtained Korringa rate ($\Delta H/\Delta T$) and g-shift (Δg) from the ESR measurements, along with the study of the macroscopic properties of $GdCuBi_2$ (e.g. specific heat data and magnetic susceptibility) made it possible to explore Gd^{3+} spin dynamics in this system based on evaluation of the exchange parameters between the Gd^{3+} ESR probes and the conduction-electrons (ce) in this compound. Our results indicate that the exchange bottleneck effects and a $\mathbf{q}$-dependent exchange interaction ($J_{fs}(\mathbf{q})$) between the $Gd^{3+}4f$ and the ce are likely to be present in $GdCuBi_2$. Disregarding the bottleneck effects in the simplest approximation, we extract the exchange parameters $J_{fs}(\mathbf{q}=0) \approx 380$ meV and $< J^2_{fs}(\mathbf{q}) >^{1/2} \approx 3.0$ meV for the Gd^{3+} spin dynamics in $GdCuBi_2$. These values of $J_{fs}(\mathbf{q})$ and $< J^2_{fs}(\mathbf{q}) >^{1/2}$ are typical of Gd^{3+} local moments in intermetallic materials and the small ratio $[< J^2_{fs}(\mathbf{q}) > / J^2_{fs}(\mathbf{0})] \approx 0.008$ suggests a strongly anisotropic (or quasi-2D) Fermi surface for $GdCuBi_2$.

1. Introduction

Complex quantum materials include several classes of intermetallic materials containing rare-earths that commonly present an intricate interplay between crystalline electrical field (CEF) effects, Ruderman–Kittel–Kasuya–Yoshida (RKKY) magnetic coupling, and Fermi surface effects.[1] In particular, the series of intermetallic compounds RTX_2 (R = Rare-earth, T = Cu and Au and X= Sb and Bi) (R-112) has been the focus of intense scientific investigation in the last decades due to the emergence of many distinct interesting physical properties such as superconductivity (SC), heavy-fermion (HF) behavior, competing anisotropic exchange interactions and CEF effects, multiple field-induced transitions, anomalous Hall effect, putative nematicity, and complex magnetic structures that were reported for this family of compounds [2–12]. Along the R-112 series, the Gd-based compounds are singular because the Gd^{3+} ions possess an S-state ($S = 7/2$, $L = 0$) ground state, which makes the CEF effects become a high order effect. Thus, the Gd-based compounds can be treated as a reference compound along a series of R-based intermetallic analogs, where the magnetic properties of the Gd-materials purely reflect important aspects of the RKKY magnetic interaction and Fermi surface effects presented in the series [11,13–20]. In addition, the Gd^{3+} ions are suitable probes for Electron Spin Resonance (ESR) studies, which can unveil important information regarding the microscopic interaction J_{fs} between the Gd^{3+} $4f$ ESR probes and the conduction electrons (ce) and the related spin dynamics of the system.

Here, we report temperature-dependent X-Band Gd^{3+} ESR in the high-T paramagnetic state of the $GdCuBi_2$ intermetallic antiferromagnetic compound. This compound presented, for $T > 250$ K, a single Dysonian Gd^{3+} ESR spectrum with a roughly temperature independent g-value and a Korringa thermal broadening of the Gd^{3+} ESR ΔH. The obtained Korringa rate ($\Delta H/\Delta T$) and g-shift (Δg) from the ESR experiments along with analysis of the specific heat and magnetic susceptibility data for $GdCuBi_2$, allowed us to investigate Gd^{3+} spin dynamics in these systems by extracting the values of the exchange parameters between the Gd^{3+} ESR probes and the ce in these compounds.

* Corresponding author at: Instituto de Física "Gleb Wataghin", UNICAMP, 13083-859, Campinas, SP, Brazil.
E-mail address: gabrielf@ifi.unicamp.br (G.S. Freitas).

https://doi.org/10.1016/j.jmmm.2024.172651
Received 11 June 2024; Received in revised form 31 October 2024; Accepted 7 November 2024
Available online 16 November 2024

The extracted values for the exchange parameters and the suggested strongly anisotropic (or quasi-2D) Fermi surface for $GdCuBi_2$ can help to understand the complex anisotropic RKKY interactions commonly observed in the $RCuBi_2$ family.

2. Experiment

Single crystals of the $GdCuBi_2$ intermetallic system were grown using the Bi-flux method [4,5]. The crystal structure and single phase character of $GdCuBi_2$ were checked by X-ray powder diffraction. This compound crystallizes in the tetragonal $P4/nmm$ structure with a stacking arrangement of GdBi-Cu-GdBi-Bi layers. Several single crystals were also submitted to elemental analysis using a commercial Energy Dispersive Spectroscopy (EDS) microprobe coupled to scanning electron microscopy. The EDS analysis revealed the stoichiometry to be close to 1:1:2 for all studied samples, namely $GdCu_{0.95(5)}Bi_2$. As such, along the text, when we referred to the compound $GdCuBi_2$, we are considering the real stoichiometry of $GdCu_{0.95(5)}Bi_2$. Furthermore, it is important to point out that the vacancies are absence of Cu atoms and cannot be directly associated with presence of Cu^{2+}. This defect could be spin-less or could have a free 1/2 spin (not obviously Cu^{2+}). From the low-T (T < 7 K) Curie tail in the magnetic susceptibility data in the Fig. 1, we estimated that the free 1/2 spin defects are not larger than 1%. As such, it is very unlikely that these free spins could give any contribution to the ESR of 100% of Gd (S = 7/2) at very high temperature.

The ESR experiments were performed in a commercial bench-top ESR spectrometer equipped with a TE_{102} cavity operated at room temperature, and temperature-dependent ESR experiments were done using a N_2 gas-flux temperature controller. Specific heat experiments were done using a commercial small-mass calorimeter, which employs a quasi-adiabatic thermal relaxation technique. The temperature-dependent magnetic susceptibility data were acquired using a commercial superconducting quantum interference device. The electrical resistivity experiments were done using a commercial low-frequency AC resistance bridge and samples mounted with a four-contact configuration. To increase the ESR signal-to-noise ratio, large $GdCuBi_2$ single crystals (several mm to cm in size) were crushed into fine powder (~ 10 μm grain size) to be used in the ESR measurements.

3. Results and discussions

Temperature dependent magnetic susceptibility taken for a magnetic field of $H = 3$ kOe applied parallel ($\chi_{//}$) and perpendicular ($\chi_{\perp}$) to the c-axis for a single crystal of $GdCuBi_2$ is shown in Fig. 1. An antiferromagnetic (AFM) phase transition can be found at $T_N = 14.3$ K for $GdCuBi_2$. In the paramagnetic state, for $T > 200$ K, Curie–Weiss (CW) linear fits of the inverse of the magnetic susceptibility, shown in the inset of Fig. 1, yield an effective moment $p = 8.1(2)\ \mu_B$ for Gd^{3+} for both directions, slightly larger than its theoretical value (7.94 μ_B). In addition, the Curie–Weiss temperature $\theta_{CW} \approx$ - 46 K ($\chi_{//}$) and $\theta_{CW} \approx$ - 36 K ($\chi_{\perp}$) extracted from the CW fits indicate the presence of magnetic frustration, with a frustration parameter $F = \theta_{CW}/T_N = 3.2$ and 2.5 for the ($\chi_{//}$) and ($\chi_{\perp}$) of $GdCuBi_2$, respectively. The temperature dependence of the magnetic susceptibility in similar conditions for the non-magnetic analog $LaCuBi_2$ is also shown for reference.

The electrical resistivity data as a function of temperature for single crystals of $GdCuBi_2$ are displayed in Fig. 2, panel 2(a). A linear metallic-like temperature dependence is observed in the paramagnetic state, and an obvious kink can be identified at the T_N values for all studied crystals. The residual resistivity ρ_0 ranged from 15–40 $\mu\Omega$cm and the RRR values within 2–3.

The magnetic specific heat per mol of Gd divided by temperature (C_m/T) and the associated magnetic entropy are presented in panel 2(b) of Fig. 2 (2 K $\lesssim T \lesssim$ 50 K) for $GdCuBi_2$. To calculate (C_m/T) and the magnetic entropy, the phonon contribution was taken into account using the specific heat data of $LaCuBi_2$ and subtracted from the total

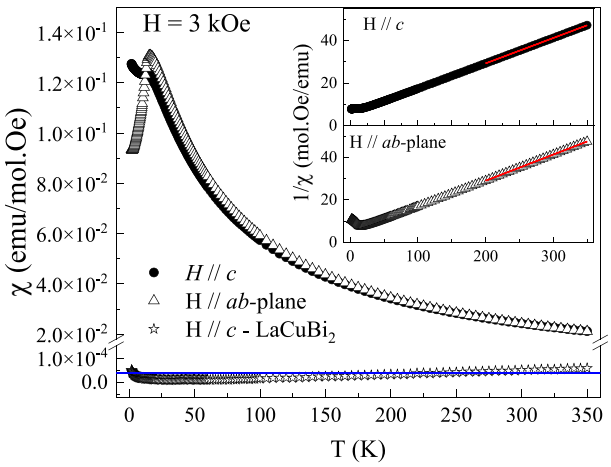

Fig. 1. Magnetic susceptibility as a function of temperature and its inverse (inset) measured with $H = 3$ kOe applied parallel ($\chi_{//}$) and perpendicular ($\chi_{\perp}$) to the c-axis for $GdCuBi_2$. The temperature dependence of the magnetic susceptibility with $H = 3$ kOe applied parallel to the c-axis for the non-magnetic analog $LaCuBi_2$ compound is also shown. The solid blue line is the calculated $\chi_e \approx 0.04 \times 10^{-3}$ emu/mol (see text) while the red lines in the inset are the Curie–Weiss fittings to the data of $GdCuBi_2$.

specific heat of the $GdCuBi_2$ system. A sharp peak-like anomaly in C_m/T is observed at $T_N = 14.3$ K in excellent agreement with the temperature of the appearance of the magnetic susceptibility maximum in Fig. 1. It is possible to identify small additional anomalies in C_m/T data around 10 K and 4 K that could be associated with a secondary magnetic phase within the ordered state or related to peculiarities of the exchange interaction and small crystal-field splitting, as frequently observed in heat capacity data of Eu^{2+} and Gd^{3+}-based magnetic intermetallic compounds with $S = 7/2$ [17,21–24]. Above T_N, the magnetic entropy reaches the value of $R\ln 8$, as expected for the Gd^{3+} $S = 7/2$ multiplet in $GdCuBi_2$ around 35 K. The fact that S does not saturate above this temperature is probably related to small discrepancies between the $GdCuBi_2$ and $LaCuBi_2$ phonon contributions.

The Gd^{3+} ESR powder spectra measured at $T = 300$ K and the temperature dependence of the Gd^{3+} ESR ΔH for $GdCuBi_2$ are displayed in Figs. 3(a) and 3(b), respectively. In the paramagnetic state, for $T > 250$ K, Dysonian [25] ESR lineshapes expected for localized ESR probes in a lattice with a skin depth smaller than the sample size were measured. By fitting the ESR spectra to the adequate admixture of absorption and dispersion [25], the Gd^{3+} ESR g-value and ΔH were extracted for $GdCuBi_2$.

For $T \gtrsim 250$ K, a single ESR line with a roughly temperature independent $g = 2.177(6)$ was found, and the Gd^{3+} ESR linewidth follows a Korringa-like linear thermal broadening as a function of temperature. At lower temperatures, the Gd^{3+} ESR ΔH starts to broaden. The Gd^{3+} ESR g-value decreases due to the emergence of AFM short-range Gd-Gd magnetic correlations in $GdCuBi_2$ (inset of Fig. 3(b)). This behavior is typically observed in the paramagnetic state for concentrated Gd- and/or Eu-based magnetically ordered materials [17–21,26]. The high-T linear ESR linewidth thermal broadening was fitted to the expression $\Delta H = a + bT$, with $a = 1760(20)$ Oe and $b = 1.0(2)$ Oe/K for $GdCuBi_2$. Using the simplest approximation to describe the exchange interaction, $J_{fs}\mathbf{S}.\mathbf{s}$, between a localized $4f$ electron spin ($\mathbf{S}$) (Gd^{3+}) and the free ce's spin ($\mathbf{s}$) of the intermetallic host, the ESR g-shift (Knight shift) [27,28] and the linewidth Korringa rate [29], when "$dynamic$" and"$bottleneck$" effects are not significant [30], can be expressed by:

$$\Delta g = J_{fs}\,\eta\left(E_F\right), \tag{1}$$

and

$$\frac{d\left(\Delta H\right)}{dT} = \frac{\pi k}{g\mu_B}\,J_{fs}^2\,\eta^2\left(E_F\right), \tag{2}$$

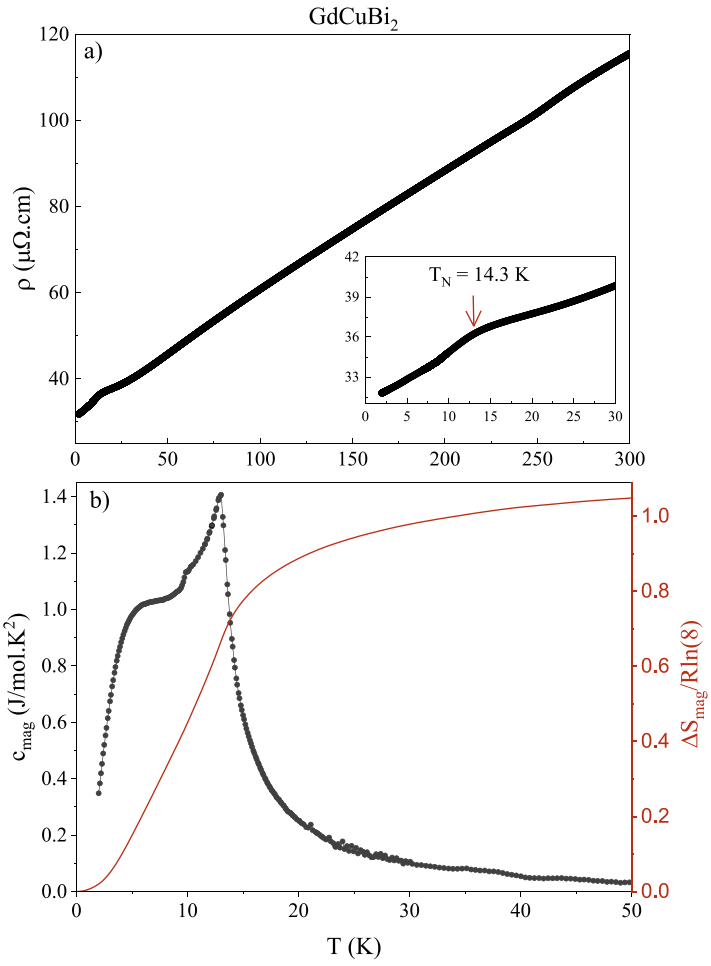

Fig. 2. Temperature dependence of (a) the electrical resistivity measured with the current applied along the [110] direction; (b) the specific heat per mole of Gd divided by temperature and the related magnetic entropy for $GdCuBi_2$.

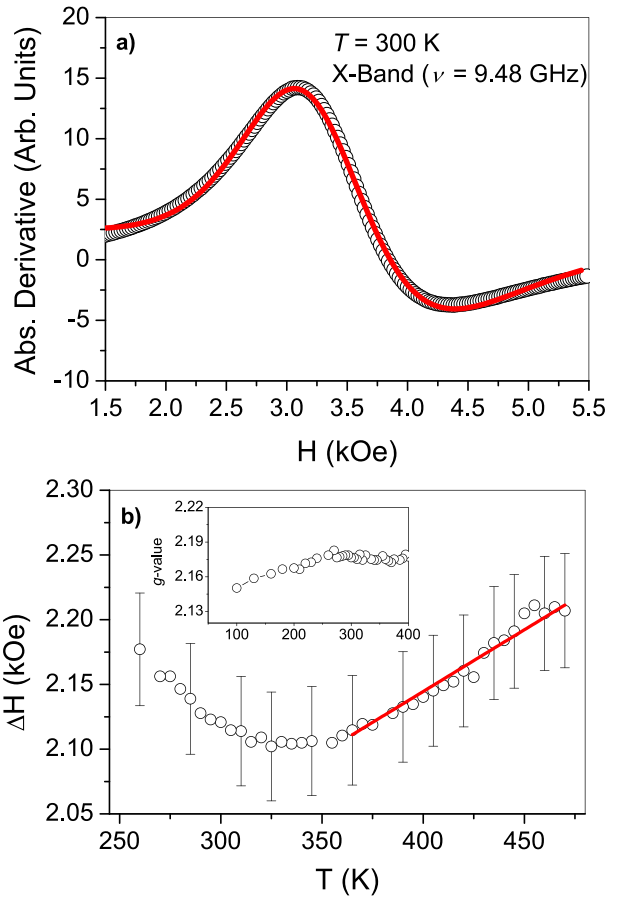

Fig. 3. (a) Gd^{3+} ESR powder spectra at $T = 300$ K with the red solid lines as the best fit of the resonance to a Dyson lineshape. (b) Temperature dependence of the ESR linewidth (and g-value in the inset) for $GdCuBi_2$. The solid red line in (b) is the best fit to $\Delta H = a + bT$, yielding a = 1760(20) Oe and b = 1.0(2) Oe/K.

where J_{fs} is the exchange interaction between the Gd^{3+} $4f$ ESR probes and the ce in the absence of ce momentum transfer [31], $\eta(E_F)$ is the "*bare*" density of states for one spin direction at the Fermi surface, μ_B is the Bohr magneton, k is the Boltzmann constant and g is the g-value for Gd^{3+}.

It important to emphasize that below 350 K, the ESR linewidth starts to broaden significantly due to the spin–spin interaction reaching values much larger than 3 kOe for the $T < 250$ K. Since this temperature range is not of interest, we choose the scales of Fig. 3(b) to show the Korringa rate at high temperature in greater detail. On the other hand, the g-value (which is the more accurate information of an ESR experiment) becomes T-dependent below ≈ 270 K, so it is useful to show the g-value data in a lower temperature range.

Eqs. (1) and (2) are usually employed to describe the ESR data for rare-earths magnetic moments highly diluted in intermetallic hosts with the presence of $c - e$ spin-flip scattering. In this situation, it might be expected that the relation below would hold:

$$\frac{d(\Delta H)}{dT} = \frac{\pi k}{g\mu_B}(\Delta g)^2, \tag{3}$$

As such, taken the g-value of Gd^{3+} in insulators as 1.993(2) [32], $(\pi k/g\mu_B) = 2.34 \times 10^4$ Oe/K, the measured g-shifts and Korringa rate, b, for the Gd^{3+} ESR in $GdCuBi_2$, after replacing $\Delta g \approx 0.184(3)$ in Eq. (3), we extract a thermal broadening of ΔH, $b \approx 790$ Oe/K. This value is, actually, much larger than the one measured, $b \approx 1.0(2)$ Oe/K. As such, one can conclude that the simplest treatment used in Eqs. 1 and 2 are not valid for a dense system such as $GdCuBi_2$, and Gd-Gd interactions, conduction electron–electron correlations [33,34], **q**-dependence of the exchange interaction, $J_{fs}(\mathbf{q})$ [31], and exchange bottleneck effects [30] may need to be considered in the analysis of the ESR data for $GdCuBi_2$".

Therefore, to further analyze our ESR data for $GdCuBi_2$, one is required to obtain the "*bare*" density of states for one spin direction at the Fermi surface, $\eta(E_F)$ for $GdCuBi_2$. Considering a free ce gas model and using the expression $\gamma = (2/3)\pi k^2 \eta(E_F)$, $\eta(E_F)$ can be extracted from the specific heat and taken into account the electronic contribution to the specific heat.

However, as can be seen in Fig. 2(b), a significant non-obvious magnon contribution to the low-T specific heat of $GdCuBi_2$ makes it difficult to estimate the correct γ value from the specific heat of $GdCuBi_2$. Alternatively, we have used the specific heat data of $LaCuBi_2$ [11] to estimate a value for $\eta(E_F)$ for $GdCuBi_2$. This is justified because both Gd^{3+} and La^{3+} are trivalent, and they similarly contribute with one $5d$ and two $6s$ electrons to the conduction band. An electronic specific heat $\gamma = 2.3(2)$ mJ/mol La-K^2 for $LaCuBi_2$ [11] yields $\eta(E_F) = 0.48(5)$ states/eV mol spin. Using this value of $\eta(E_F)$, one could extract an electronic spin susceptibility $\chi_e = 2\mu_B^2 \eta(E_F) \approx 0.04 \times 10^{-3}$ emu/mol. This value of χ_e is of the order of the Pauli susceptibility (corrected for the core-diamagnetism) obtained for $LaCuBi_2$ [11] (see Fig. 1). As such, one can disregard the conduction electron–electron correlations [33,34] in the analyses of our ESR data for $GdCuBi_2$.

Considering now the presence of a **q**-dependence of the exchange interaction in an unbottlenecked regime, $J_{fs}(\mathbf{q})$, the g-shift (Eq. (1)) and

the thermal broadening of the linewidth (Eq. (2)) may be re-written as: [30,33–35]

$$\Delta g = J_{fs}(\mathbf{0})\ \eta\left(E_F\right), \tag{4}$$

and

$$\frac{d\left(\Delta H\right)}{dT} = \frac{\pi k}{g\mu_B} < J_{fs}^2(\mathbf{q}) > \eta^2\left(E_F\right). \tag{5}$$

Using $\eta(E_F)$ = 0.48(5) states/eV mol spin and Eqs. (4) and (5), we calculated $J_{fs}(\mathbf{q}=0) \approx 380$ meV and $< J_{fs}^2(\mathbf{q}) >^{1/2} \approx 3.0$ meV for $GdCuBi_2$. This yields an exchange interaction ratio $[< J_{fs}^2(\mathbf{q}) > /J_{fs}^2(\mathbf{0})] \approx 0.008$ for $GdCuBi_2$. This value is much smaller than that found for cubic materials [36–38]. The small value of the exchange interaction ratio and the Gd^{3+} ESR positive g-shift found here suggest a strongly anisotropic (or quasi-2D) Fermi surface, with large s and d-ce contributions for $GdCuBi_2$. [39]. In fact, ESR experiments in doped $BaFe_2As_2$ could clearly provide evidence of how $< J_{fs}^2(\mathbf{q}) >^{1/2}$ can capture the dimensionality of the electronic bands in real space [39]. In particular, the Eu^{2+} ESR Korringa rate and the $< J_{fs}^2(\mathbf{q}) >^{1/2}$ were found to decrease (while $J_{fs}(0)$ remained nearly constant) as the electronic bands move further away from the Eu^{2+} sites in real space as they assume a more planar/xy-orbital character. This seems to be the case for the s and $d-ce$ electronic contributions for $GdCuBi_2$.

ESR experiments of dilute Gd^{3+} in $LaCuBi_2$ will be valuable to confirm the above results and allow the exchange bottleneck effects to be accounted for. As bottleneck effects are potentially important, the above values should be taken as a lower limit for the values of $J_{fs}(\mathbf{q})$ and $< J_{fs}^2(\mathbf{q}) >^{1/2}$ in $GdCuBi_2$.

The values of $J_{fs}(\mathbf{q})$ and $< J_{fs}^2(\mathbf{q}) >^{1/2}$ and the strongly anisotropic (or quasi-2D) with large s and d-ce contributions of $GdCuBi_2$ may help the efforts on the comprehensive study of the magnetic properties and/or the HF behavior along the R-112 series, bringing microscopic insights to the understanding of the complex RKKY magnetic interactions found in these series. [2–12].

4. Conclusions

In conclusion, we report temperature-dependent X-Band ($\nu \sim$ 9.5 GHz) Electron Spin Resonance (ESR) on the $GdCuBi_2$ intermetallic compound. This material is a metallic Curie–Weiss paramagnet at high temperature and evolves to an antiferromagnetic ordered state below T_N = 14.3 K. In the paramagnetic regime, for $T > 250$ K, a single Dysonian Gd^{3+} ESR spectrum with a roughly temperature independent g-value is observed for the studied samples. At high-T, the Gd^{3+} ESR linewidth of the $GdCuBi_2$ compound follows a Korringa-like temperature dependence. The obtained Korringa rate ($\Delta H/\Delta T$) and g-shift (Δg) from the ESR experiments supported by magnetic susceptibility and specific heat experiments for $GdCuBi_2$, allowed us to explore Gd^{3+} spin dynamics in this system and extract the exchange parameters between the Gd^{3+} ESR probes and the ce for this compound. Our results indicate a $\mathbf{q}$-dependent exchange interaction ($J_{fs}(\mathbf{q})$) between the Gd^{3+} $4f$ and the conduction electrons (ce) and exchange bottleneck effects and are likely to be present in $GdCuBi_2$. Disregarding the bottleneck effects in the simplest approximation, we could extract the exchange parameters $J_{fs}(\mathbf{q}=0) \approx 380$ meV and $< J_{fs}^2(\mathbf{q}) >^{1/2} \approx 3.0$ meV for the Gd^{3+} spin dynamics in $GdCuBi_2$.

CRediT authorship contribution statement

G.S. Freitas: Writing – review & editing, Writing – original draft, Investigation, Funding acquisition, Formal analysis, Data curation, Conceptualization. **H. Pizzi:** Investigation. **F.B. Carneiro:** Investigation. **M.H. Carvalho:** Investigation. **E.M. Bittar:** Investigation. **E.D. Bauer:** Investigation. **J.D. Thompson:** Methodology, Investigation, Formal analysis, Data curation, Conceptualization. **F. Ronning:** Investigation. **S.M. Thomas:** Investigation. **P.F.S. Rosa:** Supervision, Resources, Methodology, Investigation, Conceptualization. **S.M. Greer:** Resources, Methodology, Investigation, Funding acquisition, Data curation, Conceptualization. **P.G. Pagliuso:** Writing – review & editing, Writing – original draft, Visualization, Supervision, Resources, Project administration, Methodology, Investigation, Funding acquisition, Formal analysis, Conceptualization.

Declaration of competing interest

The authors declare that they have no known competing financial interests or personal relationships that could have appeared to influence the work reported in this paper.

Acknowledgments

We acknowledge funding from FAPESP, Brazil (grants No 2017/10581-1, 2019/26247-9, 2022/09240-3), CAPES, Brazil, CNPq, Brazil (Grants No. 405408/2023-4 and 311783/2021-0) and FINEP-Brazil. Work at Los Alamos was supported by the U.S. Department of Energy, Office of Basic Energy Sciences, Division of Materials Science and Engineering project "Quantum Fluctuations in Narrow-Band Systems".

Data availability

Data will be made available on request.

References

[1] Robert Cava, Nathalie de Leon, Weiwei Xie, Introduction: Quantum materials, Chem. Rev. 121 (2021) 2777.
[2] K.D. Myers, S.L. Bud'ko, I.R. Fisher, Z. Islam, H. Kleinke, A.H. Lacerda, P.C. Canfield, Systematic study of anisotropic transport and magnetic properties of $RAgSb_2$, (R = Y, La, Nd, Sm, Gd–Tm), J. Magn. Magn. Mater. 205 (1999) 27–52.
[3] C. Petrovic, S.L. Bud'ko, J.D. Strand, P.C. Canfield, Anisotropic properties of rare earth silver dibismites, J. Magn. Magn. Mater. 261 (2003) 210–221.
[4] C.B.R. Jesus, M.M. Piva, P.F.S. Rosa, C. Adriano, P.G. Pagliuso, Evolution of the magnetic properties along the $RCuBi_2$ (R=Ce, Pr, Nd, Gd, Sm) series of intermetallic compounds, J. Appl. Phys. 115 (2014) 17E115.
[5] C.B.R. Jesus, M.M. Piva, P.F.S. Rosa, C. Adriano, Z. Fisk, P.G. Pagliuso, Magnetic properties of the $RAuBi_2$ (R=Ce, Pr, Nd, Gd, Sm) series of intermetallic compounds, Physics Procedia 75 (2015) 618–624.
[6] S.M. Thomas, P.F.S. Rosa, S.B. Lee, S.A. Parameswaran, Z. Fisk, J. Xia, Hall effect anomaly and low-temperature metamagnetism in the Kondo compound $CeAgBi_2$, Phys. Rev. B 93 (2016) 075149.
[7] S. Seo, Xiaoyu. Wang, S.M. Thomas, M.C. Rahn, D. Carmo, F. Ronning, E.D. Bauer, R.D. dos Reis, M. Janoschek, J.D. Thompson, R.M. Fernandes, P.F.S. Rosa, Nematic State in $CeAuSb_2$, Phys. Rev. X 10 (2020) 011035.
[8] G.S. Freitas, M.M. Piva, R. Grossi, C.B.R. Jesus, J.C. Souza, D.S. Christovam, N.F. Oliveira Jr., J.B. Leão, C. Adriano, J.W. Lynn, P.G. Pagliuso, Tuning the crystalline electric field and magnetic anisotropy along the $CeCuBi_{2-x}Sb_x$ series, Phys. Rev. B 102 (2020) 155129.
[9] M.M. Piva, R. Tartaglia, G.S. Freitas, J.C. Souza, D.S. Christovam, S.M. Thomas, J.B. Leão, W. Ratcliff, J.W. Lynn, C. Lane, J.-X. Zhu, J.D. Thompson, P.F.S. Rosa, C. Adriano, E. Granado, P.G. Pagliuso, Electronic and magnetic properties of stoichiometric $CeAuBi_2$, Phys. Rev. B 101 (2020) 214431.
[10] C. Adriano, P.F.S. Rosa, C.B.R. Jesus, J.R.L. Mardegan, T.M. Garitezi, T. Grant, Z. Fisk, D.J. Garcia, A.P. Reyes, P.L. Kuhns, R.R. Urbano, C. Giles, P.G. Pagliuso, Physical properties and magnetic structure of the intermetallic $CeCuBi_2$ compound, Phys. Rev. B 90 (2014) 235120.
[11] G.S. Freitas, S.G. Mercena, C.B.R. Jesus, C. Adriano, M.M. Piva, J.C. Souza, H.B. Pizzi, A.M. Caffer, F.B. Carneiro, M.H. Carvalho, C. Girod, M.M. Bordelon, X. Gratens, E.D. Bauer, F. Ronning, J.D. Thompson, S.M. Thomas, Z. Fisk, N.F. Oliveira Jr., D.J. Garcia, P.F.S. Rosa, P.G. Pagliuso, De Gennes scaling breakdown in the $RTBi_2$ (R=Ce, Pr, Nd; T=Cu, Au) series: the role of crystal field effects and anisotropic magnetic interactions, Phys. Rev. B (2024) submitted for publication.
[12] M.M. Bordelon, C. Girod, F. Ronning, K. Rubi, N. Harrison, J.D. Thompson, C. dela Cruz, S.M. Thomas, E.D. Bauer, P.F.S. Rosa, Interwoven atypical quantum states in $CeLiBi_2$, Phys. Rev. B 106 (2022) 214433.
[13] P.G. Pagliuso, J.D. Thompson, M.F. Hundley, J.L. Sarrao, Z. Fisk, Crystal structure and low-temperature magnetic properties of R_mMIn_{3m+2} compounds (M = Rh or Ir; m = 1,2; R=Sm or Gd), Phys. Rev. B 63 (2001) 054426.

[14] E. Granado, P.G. Pagliuso, C. Giles, R. Lora-Serrano, F. Yokaichiya, J.L. Sarrao, Magnetic structure and fluctuations of Gd_2IrIn_8: A resonant x-ray diffraction study, Phys. Rev. B 69 (2004) 144411.

[15] E. Granado, B. Uchoa, A. Malachias, R. Lora-Serrano, P.G. Pagliuso, H. Westfahl Jr., Magnetic structure and critical behavior of $GdRhIn_5$: Resonant x-ray diffraction and renormalization group analysis, Phys. Rev. B 74 (2006) 214428.

[16] A. Malachias, E. Granado, R. Lora-Serrano, P.G. Pagliuso, C.A. Pérez, H. Westfahl Jr., Spin structure and first-order transition of $GdIn_3$: Near-surface magnetism, buried amplitude-modulated phase, and interface delocalization, Phys. Rev. B 77 (2008) 094425.

[17] C.B.R. Jesus, P.F.S. Rosa, T.M. Garitezi, G.G. Lesseux, R.R. Urbano, C. Rettori, P.G. Pagliuso, Electron spin resonance of the half-Heusler antiferromagnet GdPdBi, Solid State Commun. 177 (2014) 95.

[18] M.A. Pires, L. Mendonça Ferreira, J.G.S. Duque, R.R. Urbano, O. Agüero, I. Torriani, C. Rettori, E.M. Bittar, P.G. Pagliuso, Crystal structure and physical properties of $Gd_3Co_4Sn_{13}$ intermetallic antiferromagnet, J. Appl. Phys. 99 (2006) 08J311.

[19] J.G.S. Duque, C. Adriano, R. Lora-Serrano, C. Rettori, R.R. Urbano, J.L. Sarrao, S.B. Oseroff, P.G. Pagliuso, Electron spin resonance of Gd^{3+} in $Gd_m M_nIn_{3m+2n}$ (M = Rh,Ir; n = 0,1; m = 1,2) antiferromagnets, J. Appl. Phys. 103 (2008) 07B733.

[20] J.G.S. Duque, E. Miranda, A.M.O. Belon, L. Bufaiçal, C. Rettori, P.G. Pagliuso, Magnetic properties of frustrated Y-doped $GdInCu_4$, Physica B 398 (2007) 430.

[21] P.G. Pagliuso, J.L. Sarrao, J.D. Thompson, M.F. Hundley, M.S. Sercheli, R.R. Urbano, C. Rettori, Z. Fisk, S.B. Oseroff, Antiferromagnetic ordering of divalent Eu in $EuCu_2Si_2$ single crystals, Phys. Rev. B 63 (2001) 092406.

[22] M. Bouvier, P. Lethuillier, D. Schmitt, Specific heat in some gadolinium compounds. I. Experimental, Phys. Rev. B 43 (1991) 13137.

[23] S. Süllow, I. Prasad, M.C. Aronson, J.L. Sarrao, Z. Fisk, D. Hristova, A.H. Lacerda, M.F. Hundley, A. Vigliante, D. Gibbs, Structure and magnetic order of EuB_6, Phys. Rev. B 57 (1998) 5860.

[24] M. Radaelli, M.M. Piva, J.C. Souza, G.G. Lesseux, C.B.R. Jesus, D. Tobia, R.R. Urbano, P.F.S. Rosa, P.G. Pagliuso, Probing putative orbital differentiation effects via Eu^{2+} spin dynamics in $Sr_{1-x}Eu_xFe_2As_2$, Phys. Rev. B 107 (2023) 134512.

[25] F.J. Dyson, Electron spin resonance absorption in metals. II. Theory of electron diffusion and the skin effect, Phys. Rev. 98 (1955) 349.

[26] P.F.S. Rosa, C. Adriano, T.M. Garitezi, R.A. Ribeiro, Z. Fisk, P.G. Pagliuso, Electron spin resonance of the intermetallic antiferromagnet $EuIn_2As_2$, Phys. Rev. B 86 (2012) 094408.

[27] K. Yosida, Magnetic properties of Cu-Mn alloys, Phys. Rev. 106 (1957) 893.

[28] P.G. Pagliuso, C. Rettori, J.L. Sarrao, A. Cornelius, M.F. Hundley, Z. Fisk, S.B. Oseroff, Electron spin resonance of Gd^3+ and Nd^3+ in $LuInA_4$ (A=Cu, Ni), Phys. Rev. B 60 (1999) 13515.

[29] J. Korringa, Nuclear magnetic relaxation and resonnance line shift in metals, Physica 16 (1950) 601.

[30] C. Rettori, H.M. Kim, E.P. Chock, D. Davidov, Dynamic behavior of paramagnetic ions and conduction electrons in intermetallic compounds: $Gd_xLu_{1-x}Al_2$, Phys. Rev. B 10 (1974) 1826.

[31] D. Davidov, K. Maki, R. Orbach, C. Rettori, E.P. Chock, Electron spin resonance of Gd in the intermetallic compounds YCu, YAg, and LaAg: Wave vector dependence of the exchange interaction, Solid State Commun. 12 (1973) 621.

[32] A. Abragam, B. Bleaney, EPR of Transition Ions, Clarendon Press, Oxford, 1970.

[33] T. Moriya, The effect of electron-electron interaction on the nuclear spin relaxation in metals, J. Phys. Soc. Japan 18 (1963) 516.

[34] A. Narath, Nuclear magnetic resonance and relaxation of ^{197}Au in gold metal and ^{109}Ag in gold-silver alloys, Phys. Rev. 163 (1967) 232.

[35] D. Davidov, R. Orbach, C. Rettori, D. Shaltiel, L.J. Tao, B. Ricks, Hyperfine splitting in the electron spin resonance of Dy and Er in the transition metal-Rh, Phys. Lett. A 35 (1971) 339.

[36] P.G. Pagliuso, C. Rettori, S.B. Oseroff, J. Sarrao, Z. Fisk, A. Cornelius, M.F. Hundley, ESR of Gd^3+ in the Kondo-lattice compound $YbAgCu_4$ and its reference compounds $RAgCu_4$ (R = Y, Lu), Phys. Rev. 56 (1997) 8933.

[37] C. Rettori, S.B. Oseroff, D. Rao, P.G. Pagliuso, G.E. Barberis, J. Sarrao, Z. Fisk, M. Hundley, ESR of Gd^{3+} in the intermediate-valence $YbInCu_4$ and its reference compound $YInCu_4$, Phys. Rev. B 55 (1997) 1016.

[38] E.M. Bittar, C. Adriano, C. Giles, C. Rettori, Z. Fisk, P.G. Pagliuso, Probing the localized to itinerant behavior of the 4f electron in $CeIn_{3-x}Sn_x$ by Gd^{3+} electron spin resonance, Phys. Rev. B 86 (2012) 125108.

[39] P.F.S. Rosa, C. Adriano, T.M. Garitezi, T. Grant, Z. Fisk, R.R. Urbano, P.G. Pagliuso, Site-specific spin dynamics in $BaFe_2As_2$: tuning the ground state by orbital differentiation, Sci. Rep. 4 (2014) 6543, For a better understanding of this reasoning, please see, and references therein.